

Least-squares migration using surface-related multiples on data with large acquisition gaps

Verschuur, D.J.; Nath, Aparajita

DOI

[10.3997/2214-4609.201803067](https://doi.org/10.3997/2214-4609.201803067)

Publication date

2018

Document Version

Final published version

Published in

Least-squares migration using surface-related multiples on data with large acquisition gaps

Citation (APA)

Verschuur, D. J., & Nath, A. (2018). Least-squares migration using surface-related multiples on data with large acquisition gaps. In *Least-squares migration using surface-related multiples on data with large acquisition gaps* EAGE. <https://doi.org/10.3997/2214-4609.201803067>

Important note

To cite this publication, please use the final published version (if applicable). Please check the document version above.

Copyright

Other than for strictly personal use, it is not permitted to download, forward or distribute the text or part of it, without the consent of the author(s) and/or copyright holder(s), unless the work is under an open content license such as Creative Commons.

Takedown policy

Please contact us and provide details if you believe this document breaches copyrights. We will remove access to the work immediately and investigate your claim.

47074

Least-Squares Migration Using Surface-Related Multiples on Data with Large Acquisition Gaps

A. Nath* (Delft University of Technology), D.J. Verschuur (Delft University of Technology)

Summary

Seismic acquisition in an area can often get hindered by reasons such as complex topography, infrastructure (e.g. platforms) or lack of access due to legal and environmental reasons. Such areas with possibilities of large data gaps may deter exploration or monitoring, as the conventional imaging strategies would either provide bad seismic images or turn out to be very expensive. Surface-related multiples travel different paths compared to primaries, illuminating a wider subsurface area. This property makes the surface-related multiples particularly important in case of data with large gaps. In this paper we show different strategies of using surface-related multiples to get around the problem of imaging with a large data gap. Conventional least-squares imaging methods that incorporate surface-related multiples do so by re-injecting the measured wavefield, which makes it sensitive to missing data. Therefore, we present a 'non-linear' imaging method that models all the surface-related multiples in the unacquired section from the original source field. Eventually we also demonstrate a 'hybrid' method that combines the 'non-linear' imaging method with the conventional 'linear' multiple imaging method, which further improves our imaging result. We test the methods on synthetic as well as field data. Despite large acquisition gaps, our method gives promising results.

Introduction

In this article we are primarily pursuing the following two questions; 1) how do we get a good seismic image despite large gaps in the data, and 2) how do we reduce the dependency of the current migration methods that use surface-related multiples on good receiver coverage.

The first question stems from the often stumbled upon problem, where we end up with huge data gaps due to reasons like complex topography, platforms, lack of access etc. Imaging using such inadequate data leads to migration artefacts. A common solution in such cases is re-acquiring the data around the area with missing data, which makes the process more time consuming and expensive. Therefore, an ideal solution would be to reduce such expense by using the already existing data to get a good image.

Migration with surface-related multiples provide much wider subsurface illumination than the migration of primaries (Berkhout and Verschuur, 1994; Tu *et al.* 2011; Guitton, 2002), which makes it a viable solution to our first problem. In one of the methods, Verschuur and Berkhout (2011) proposed using the *complete downgoing wavefield*, comprising of the source wavefield and the downward reflected total wavefield at the surface as the illuminating source wavefield for the total measured response. This helps in integrating the surface-related multiples in imaging as primaries and multiples are simultaneously migrated. However, since this method relies on reinjection of recorded data as incident wavefield, it becomes sensitive to incomplete seismic data. This brings us to the second problem stated above.

In the next sections, we present a ‘non-linear’ imaging scheme where instead of re-injecting the recorded data, we incrementally model all the surface-related multiples, starting from the original source wavefield. In this way the dependence on receiver geometry becomes less strong, allowing us to overcome large acquisition gaps, thereby solving both our problems. We also discuss a hybrid method that combines the existing methods along with the ‘non-linear’ imaging scheme. We demonstrate this methodology on finite-difference data as well as field data from the Vøring basin.

Theory

Imaging methods using surface-related multiples

To include surface-related multiples in a migration scheme, slight modifications are required in the forward modeling process. One of the ways is to include a secondary source in the form of re-injected total measured wavefield along with the original source wavefield $\vec{S}^+(z_0)$ ¹. The new incident wavefield or the ‘total downgoing wavefield’ $\vec{Q}^+(z_0)$ is given by:

$$\vec{Q}^+(z_0) = \vec{S}^+(z_0) + \mathbf{R}^\cap(z_0, z_0)\vec{P}^-(z_0), \quad (1)$$

where $\vec{P}^-(z_0)$ refers to the total ‘recorded’ wavefield at the acquisition surface and $\mathbf{R}^\cap(z_0, z_0)$ represents the downward reflectivity operator at the surface z_0 (Verschuur and Berkhout, 2011). Using the one way wavefield propagation operators \mathbf{W}^+ and \mathbf{W}^- (see Berkhout, 1982), the forward extrapolated downgoing wavefield $\vec{P}^+(z_m, z_0)$ and the backward extrapolated upgoing wavefield $\vec{P}^-(z_m, z_0)$ at the depth level z_m from z_0 are given by:

$$\vec{P}^+(z_m, z_0) = \mathbf{W}^+(z_m, z_0)\vec{Q}^+(z_0), \quad (2)$$

$$\begin{aligned} \vec{P}^-(z_m, z_0) &= [\mathbf{W}^-(z_0, z_m)]^{-1}\vec{P}^-(z_0) \\ &\approx [\mathbf{W}^+(z_m, z_0)]^*\vec{P}^-(z_0). \end{aligned} \quad (3)$$

This method now becomes similar to imaging with primary wavefield since the re-injected wavefield is used to explain the surface-related multiples in next order of scattering. This leads to a ‘linear’ relationship between the forward model and the reflectivity (the effect of internal multiples is excluded). Reflectivity can now be obtained using one of the traditional imaging principles (e.g. by the correlation of $\vec{P}^+(z_m, z_0)$ and $\vec{P}^-(z_m, z_0)$), migrating the primaries and multiples simultaneously (Berkhout and Verschuur, 1994). Since conventional imaging conditions are not equipped to handle complex re-injected wavefield, it is replaced by a least-squares minimization process with an iterative inversion method (or

¹For the used matrix notation kindly refer to Berkhout (1982).

closed-loop method) (Davydenko and Verschuur, 2012). The cost function J_i of the iterative minimization process is given by:

$$J_i = \sum_{shots} \sum_{\omega} \|\vec{P}^-(z_0) - \mathbf{W}^-(z_0, z_m) \mathbf{R}_i^U \vec{P}^+(z_m, z_0)\|^2. \quad (4)$$

For a given iteration i , the current reflectivity operator matrix \mathbf{R}_i^U , is used to forward model seismic data using the propagation operators, after which this modeled data is compared to the measured data. The residual data is then used to update the reflectivity, thereby also suppressing possible cross-talk. This method can successfully overcome the limitations of coarse source sampling (see e.g. Lu *et al.* 2014). However, as the recorded wavefield becomes the incident wavefield for imaging, the performance of the method is dependent on good receiver coverage and density.

Incorporating surface multiples in a ‘non-linear’ inversion method

To overcome the limitations mentioned in the previous section, we suggest the ‘non-linear’ inversion scheme. In this method, instead of re-injecting the measured wavefield, all the surface-related multiples are modeled incrementally using an initial source wavefield. This leads to a non-linear relationship between reflectivity and the forward model. Since this method omits the re-injection of measured data, it is less affected by the missing data.

In this method we forward model with $\vec{S}^+(z_0)$ as our initial incident wavefield. In subsequent iterations, we modify the downgoing wavefield $[\vec{Q}^+(z_0)]^i$ such that it includes the modeled surface multiples, based on re-injection of the *modeled* upgoing wavefield from the previous iteration. Therefore, $[\vec{Q}^+(z_0)]^i$ when only considering free surface reflections is given by:

$$[\vec{Q}^+(z_0)]^i = \vec{S}^+(z_0) + \mathbf{R}^\cap(z_0) [\vec{P}_m^-(z_0, z_0)]^{i-1}; \quad (5)$$

here i refers to the iteration number. After making suitable changes for ‘non-linear’ imaging in the closed loop approach, we then derive the reflectivity image using equation 4.

Hybrid approach

Although the ‘non-linear’ method performs better in case of incomplete sampling, it has few drawbacks of its own. As the data is modeled from the source wavefield, it is not as robust as the ‘linear’ method. The relationship between the forward model and reflectivity is non-linear, hence this method is also more sensitive to errors. Moreover, unlike the ‘linear’ imaging method, the ‘non-linear’ imaging method requires knowledge of the source wavefield. Since the ‘linear’ and ‘non-linear’ methods complement each other on their drawbacks and benefits, a better approach would be to combine the two methods in a hybrid approach by successively implementing the methods. In our strategy, we first start with the ‘non-linear’ imaging method process since it does a better job at modeling data in the gap. Then we use the modeled shot record gather from non-linear inversion method to fill in the gaps of the measured seismic data. As the ‘linear’ inversion method is more robust, we use this infilled data in the ‘linear’ inversion method to obtain an intermediate subsurface image. Finally, as the ‘non-linear’ inversion method explains the missing data better, we feed this reflectivity image received after the ‘linear’ inversion method as a jump start to the ‘non-linear’ inversion method along with the original measured data. This provides the final image.

Examples

Synthetic Data Examples

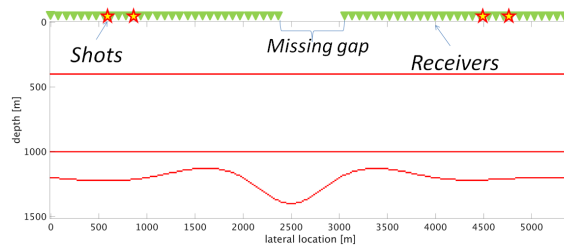


Figure 1 Synthetic model with four sources at 600 m, 900 m, 4500 m and 4800 m (indicated by red stars). Receivers (indicated by green triangles) are spread throughout the surface except from $x=2400$ m to $x=3000$ m.

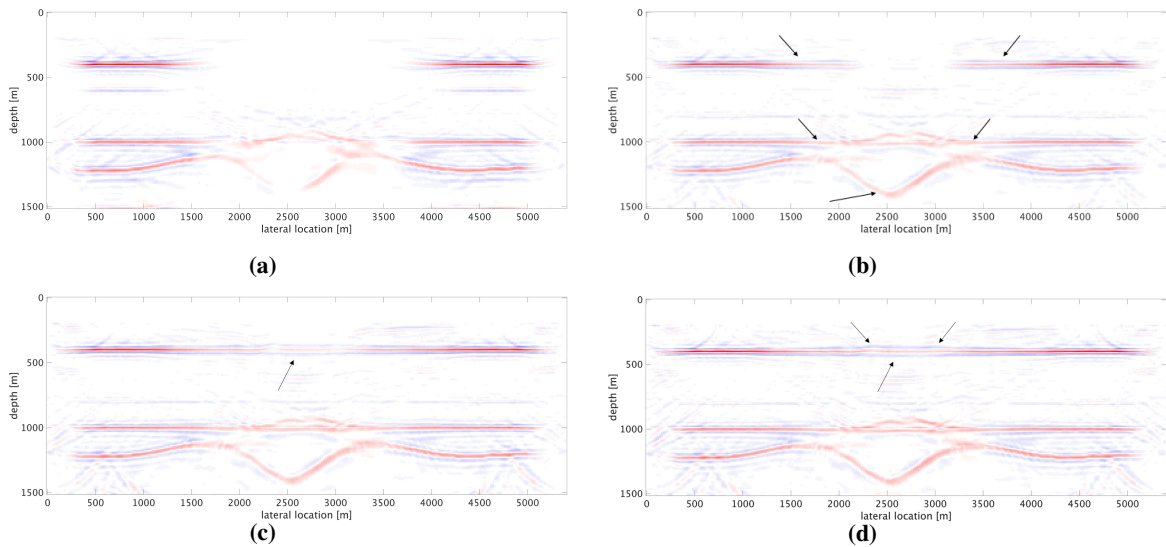


Figure 2 Imaging results based on finite-difference modelled input data: a) using primaries; b) using multiples in a ‘linear’ imaging method; c) using the proposed non-linear inversion method; d) final result of the hybrid method. Residual data for the source at 900 m for: a) the linear inversion method; b) the final hybrid scheme.

Here we illustrate the different methods using a synthetic model (see figure 1) of size 1500 m in depth by 5400 m horizontally. We have put only four sources in this example. In order to imitate a wide receiver gap, receivers have been put throughout the surface at an interval of 20 m except from $x=2400$ m to $x=3000$ m. In this example, synthetic data is generated using acoustic finite difference modeling. Figure 2a shows the imaging result using the primaries only data. The effects in the image due to missing receivers is clearly visible. While, figure 2b shows the imaging result using primaries and multiples via the closed-loop linear inversion method mentioned earlier. Upon comparison with figure 2a, the benefits of using the free-surface multiples is already visible here. The improvements in the image can be noticed not only at the shallowest reflector but also in the deeper reflectors. Figure 2c illustrates the imaging result from the ‘non-linear’ imaging method. The shallowest reflector can be seen better imaged around the area with the receiver gap (marked with arrows). Figure 2d shows the final imaging result obtained via the hybrid method. A considerable improvement is seen upon comparison of image in figure 2d with figure 2a or figure 2b. Improvements were also seen in the residual data from the hybrid method to the one from the ‘linear’ method indicating better modeling of data.

Field Data example

In this section we compare these methods on field data from the Vøring basin. We select a subset over 5800 m of recording and use four shot records with sources at 1600 m, 2100 m, 3600 m and 4100 m. Receivers are spread along the surface at a spacing of 25 m except from $x=2600$ m to $x=3600$ m, yielding a 1 km receiver gap. Figure 3e shows one of these shot records. Figure 3a shows the imaging result using the closed-loop ‘linear’ inversion method. The effects in the image due to missing receivers can be seen in the area marked with arrows. Figure 3b shows the final imaging result of the hybrid approach. The reflectors can be seen better imaged not only around the area with gap, but also in the far offsets (marked with arrows). Figure 3c and 3d are the enlarged sections of figure 3a and 3b respectively in the area with most upliftment of the image. Finally, in figure 3f we display the same shot record as figure 3e with the reconstructed data in the gap. Although the reconstruction for the surface multiples (starting at $t=4$ seconds) is somewhat weaker, we see a proper reconstruction of the primaries. Note that this information originated from the multiples.

Conclusions

We set out to tackle the problem of imaging in case of large acquisition gaps using surface-related multiples. We thereby introduce the ‘non-linear’ imaging method, that performs quite well

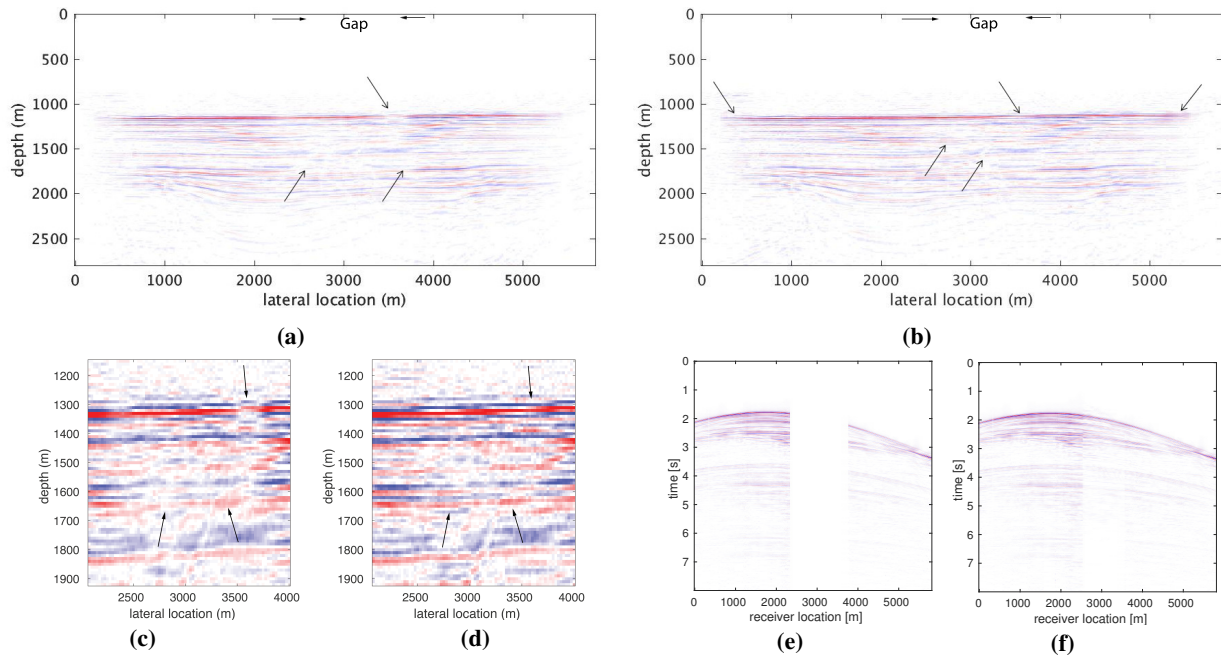


Figure 3 Imaging results for a geometry with only four sources: a) using multiples in a linear imaging method, b) final result of the hybrid method. c) An enlarged section from $x=2075$ m to 4000 m from figure 3a and d) the same enlarged section from figure 3b. d) Measured shot record data for the source at 2100m, e) Data after putting an infill in the gap received from non-linear inversion.

despite large acquisition gaps. This method is less dependent on receiver density as it is based on forward modeling of all the surface-related multiples from the original source wavefield instead of re-injecting the measured data. The method uses non-linear forward modeling of data, making it sensitive to inaccurate velocity models. We further demonstrate a hybrid method that combines the ‘linear’ and ‘non-linear’ imaging methods in order to get the best features of both the methods while also tackling their limitations. The merits of this approach have been demonstrated with success on synthetic and field data.

Acknowledgements

The authors would like to thank all the sponsors of the Delphi consortium for their support and Statoil for providing the field data.

References

- Berkhout, A.J. [1982] *Seismic migration, imaging of acoustic energy by wave field extrapolation, A: theoretical aspects*. Elsevier (second edition).
- Berkhout, A.J. and Verschuur, D.J. [1994] Multiple technology: Part 2, migration of multiple reflections. In: *SEG Technical Program Expanded Abstracts*, Society of Exploration Geophysicists, 1497–1500.
- Davydenko, M. and Verschuur, D.J. [2012] Demonstration of full wavefield migration in 2D subsurface models. In: *Extended abstracts*. P275.
- Guitton, A. [2002] Shot-profile migration of multiple reflections. In: *SEG Technical Program Expanded Abstracts 2002*, Society of Exploration Geophysicists, 1296–1299.
- Lu, S., Whitmore, D.N., Valenciano, A.A. and Chemingui, N. [2014] Separated-wavefield imaging using primary and multiple energy. *First Break*, **32**(11), 87–92.
- Tu, N., Lin, T.T., Herrmann, F.J. et al. [2011] Migration with surface-related multiples from incomplete seismic data. In: *2011 SEG Annual Meeting*. Society of Exploration Geophysicists.
- Verschuur, D.J. and Berkhout, A.J. [2011] Seismic migration of blended shot records with surface-related multiple scattering. *Geophysics*, **76**(1), A7–A13.